Jones, Mitchell; Weiland, Kathrin; Kujundzic, Marina; Theiner, Johannes; Kählig, Hanspeter; Kontturi, Eero; John, Sabu; Bismarck, Alexander; Mautner, Andreas

Waste-Derived Low-Cost Mycelium Nanopapers with Tunable Mechanical and Surface Properties

Published in:
Biomacromolecules

DOI:
10.1021/acs.biomac.9b00791

Published: 01/01/2019

Document Version
Peer-reviewed accepted author manuscript, also known as Final accepted manuscript or Post-print

Waste-derived Low-cost Mycelium Nanopapers with Tunable Mechanical and Surface Properties

Mitchell Jones[a,b], Kathrin Weiland[b], Marina Kujundzic[b], Johannes Theiner[c], Hanspeter Kählig[d], Eero Kontturi[e], Sabu John[a], Alexander Bismarck[b,f], Andreas Mautner[b]*

[a] School of Engineering, RMIT University, Bundoora East Campus, PO Box 71, Bundoora 3083, VIC, Australia
[b] Institute of Material Chemistry and Research, Polymer and Composite Engineering (PaCE) Group, Faculty of Chemistry, University of Vienna, Währinger Straße 42, 1090, Vienna, Austria
[c] Microanalytical Laboratory, Institute of Physical Chemistry, Faculty of Chemistry, University of Vienna, Währinger Straße 42, 1090, Vienna, Austria
[d] Institute of Organic Chemistry, Faculty of Chemistry, University of Vienna, Währinger Strasse 38, 1090 Vienna, Austria
[e] Department of Bioproducts and Biosystems (BIO^2), PO Box 16300, FI-00076, Aalto University, Finland.
[f] Polymer & Composite Engineering (PaCE) Group, Department of Chemical Engineering, Imperial College London, South Kensington Campus, London, SW7 2AZ, UK
* Corresponding author. *Email address*: andreas.mautner@univie.ac.at (A. Mautner).

Abstract

Mycelium, the vegetative growth of filamentous fungi, has attracted increasing commercial and academic interest in recent years due to its ability to upcycle agricultural and industrial wastes into low-cost, sustainable composite materials. However, mycelium composites typically exhibit foam-like mechanical properties, primarily originating from their weak organic filler constituents. Fungal growth can be alternatively utilised as a low-cost method for on-demand generation of natural nanofibrils, such as chitin and chitosan, which can be grown and isolated from liquid wastes and by-products in the form of fungal micro-filaments. This study characterised polymer extracts and nanopapers produced from a common mushroom reference and various species of fungal mycelium grown on the sugarcane by-product molasses. Polymer yields of ~10-26% were achieved, which is comparable to those of crustacean-derived chitin, and the nanopapers produced exhibited much higher tensile strengths than existing mycelium materials, with values of up to ~25 MPa (mycelium) and ~98 MPa (mushroom), in addition to useful hydrophobic surface properties resulting from the presence of organic lipid residues in the nanopapers. HCl or H_2O_2 treatments were used to remove these impurities facilitating tuning of mechanical, thermal and surface properties of the nanopapers produced. This potentially enables their use in a wide range of applications including coatings, membranes, packaging and paper.

Keywords: Mycelium, waste upcycling, wettability, chitin, chitosan

1. Introduction

The vegetative growth of filamentous fungi (mycelium) has attracted increasing academic and commercial interest over the past decade as a natural binder for packaging, acoustic and thermal insulation and textile materials.[1-5] Mycelium binds organic matter through a network of hyphal micro-filaments in a natural biological process which allow them to be exploited to produce useful composite materials.[1-2, 6-8] Mycelium-derived materials have several key advantages over traditional synthetic materials including their low cost, low environmental impact and carbon footprint, reduced energy consumption and biodegradability.[6, 9-10] Unfortunately, mycelium-derived materials are typically limited to mechanical properties resembling foams and natural materials. Mycelium composites comprise a combination of fungal mycelium and undigested lignocellulosic material and have foam-like mechanical properties with ultimate tensile strengths of up to 1.1 MPa.[6] Conversely, mycelial biomass comprises only fungal mycelium and exhibits material properties typical of natural materials, such as wood and cork, with tensile strengths up to 9.6 MPa for *Schizophyllum commune*.[11] Limitations in the strength of mycelium composites result from the often low-strength agricultural waste or by-products utilised in these composites as filler, which are weakly bonded by a hyphal filament matrix,[3] while the strength of mycelium itself is limited by the presence of non-structural elements, such as cytoplasm, proteins and lipids present in the fungal biomass.[12]

The mechanical performance of mycelium-derived materials can be improved by eliminating the use of these low-strength wastes and by-products as composite fillers, instead utilising them solely as nutrient sources for fungal growth and removing non-structural elements from the isolated mycelium. This process constitutes the conversion of agricultural biomass into natural polymers within fungal biomass, such as nitrogenous polysaccharide-based chitin nanofibers, that can be extracted from the cell walls of hyphae within the mycelial biomass. Chitin is a linear macromolecule composed of acetylated N-acetylglucosamine that is also the main component of the exoskeleton of most insects and other arthropods.[13] It is strong with a nanofibril tensile strength of ~1.6-3.0 GPa[14] due to hydrogen bonding along the chains which give them rigidity.[15]

Mycelium-derived chitin offers a cheap, renewable, easily isolated and abundant alternative to more expensive, seasonally and regionally limited, allergenic crustacean chitin.[16-18] The fungal chitin structure is also associated with more pliable branched β-glucan or chitosan, providing a native nanocomposite architecture that is both strong and tough.[19] Chitin derived from mycelium is also more viable than fungal chitin derived from mushrooms, which takes

much longer to grow and if derived from edible mushrooms is more expensive, directly competing with food supply.

This study aimed to produce nanopapers produced from mycelium-derived chitin-glucan or chitin-chitosan exhibiting better mechanical properties than existing mycelium materials. Emphasis was on cost and environmental impact with only cheap agricultural by-products and natural fungal growth used to obtain chitinous fungal biomass. Structural polymers, such as chitin and chitosan, were then extracted from this fungal biomass using simple alkaline treatment, followed by vacuum filtration and hot-pressing to produce homogenous nanopapers. The morphology, composition and molecular structure of the nanopapers were then analysed in addition to their physical, mechanical and surface properties.

2. Experimental section

2.1 Materials

Allomyces arbuscula and *Mucor genevensis* were obtained from the RMIT University fungal culture collection (Bundoora, Australia). The cultures were stored under oil on a nutrient agar slope, which was subcultured onto fresh sterile malt extract agar (Neogen, Michigan) plates and incubated inverted at 25°C in darkness for 7 d. *Trametes versicolor* was purchased from New Generation Mushroom Supplies (Melbourne, Australia). The sample was supplied as mycelium on wheat grain sealed in a plastic bag with a filter patch. This isolate was subcultured onto malt extract agar plates and incubated as above. *Agaricus bisporus* (white button) mushrooms were purchased from a local convenience store (origin: B. Fungi Kft, Ocsa, Hungary). Blackstrap molasses was purchased from Nortem Biotechnology (El Puerto de Santa Maria, Spain). NaOH (≥ 97.0%), H_2O_2 (34.5-36.5%) and HCl (37% ACS reagent) were purchased from Sigma-Aldrich. Deionised water was used for all experiments.

2.2 Species and medium selection

Fungal species were selected for use in this study based on their fibrillar structural polymers, biosafety level, hyphal branching and growth performance **(Table 1)**. Fibrillar cell wall polymers, such as chitin, chitosan and glucan, were of primary interest in this study, but it should be noted that cell walls also contain polysaccharides (e.g. galactose, mannose and fucose), phosphate, proteins, lipids and mineral salts.[12] *T. versicolor* is a widely available trimitic white-rot fungus containing chitin and glucan fibrillar cell wall polymers. It is commonly used in mycelium-based materials science applications[3, 6, 20] and is known to have a high growth rate and biomass yield.[21] *A. arbuscula* also comprises a chitin-glucan cell wall structure but has been noted to have a much higher cell wall chitin content than other fungi.[22] It is also sympodially/dichotomously branched giving it a higher growth rate than the sympodially/monopodially branched *M. genevensis*, which was selected for its chitin-

chitosan cell wall structure rather than its growth rate. Only safe species (biosafety level 1) were used in this study. The mycelium (vegetative root like structure) of these species was grown on the sugarcane by-product blackstrap molasses, an exceptional fungal nutrient with biomass yields comparable or better than those of commonly used laboratory nutrient malt extract.[23] Production of mycelial biomass from blackstrap molasses constituted a sustainable and rapid upcycling of low-cost liquid waste into chitin-glucan or chitin-chitosan fibrillar polymers, which could directly compete with more expensive crustacean and fruiting body (mushroom) derived chitin. The common white button mushroom (*A. bisporus* fruiting body) was also included in this study for reference **(Table 1)**.

Table 1. Fungal species used in this study by biomass component utilised, polymers present in cell wall, biosafety level and hyphal branching type. Compiled from Kavanagh,[12] Webster and Weber,[15] American Type Culture Collection,[24] Bioresource Collection and Research Center,[25] and U.S. Department of Health and Human Services.[26]

Species	Biomass	Fibrillar polymers	Hyphal branching	Biosafety
A. bisporus	Fruiting body	Chitin-glucan	Monomitic	1
A. arbuscula	Mycelium	Chitin-glucan	Sympodially/dichotomously	1
M. genevensis	Mycelium	Chitin-chitosan	Sympodially/monopodially	1
T. versicolor	Mycelium	Chitin-glucan	Trimitic	1

2.3 Fungal growth

Molasses liquid media were prepared by diluting blackstrap molasses using water (1 g/10 mL) and autoclaving at 121°C for 20 min. Shallow liquid bodies (approximately 100 mL) were aseptically dispensed into 1 L glass vessels. Isolate cultures of each fungal species were cut into inoculum disks with a diameter of 7 mm and suspended in the liquid media, which was left at room temperature (25°C) for 14 d on an IKA® KS260 Basic orbital shaker at 50 rpm. The resulting mycelia (fungal biomass) were then washed with water and vacuum filtered (VWR 125 mm qualitative filter paper 413, particle retention 5-13 µm) to remove any excess water. The total wet biomass quantity ($WM_{Fungal\ biomass}$) was assessed using a laboratory balance. Triplicate 50 mg samples were then removed from the wet biomass and weighed pre- (wet mass, WM_{Sample}) and post-drying (dry mass, DM_{Sample}) at 105°C for 12 h using a Sartorius Cubis® micro-balance. The water content of each sample was calculated, and the average water content ($\overline{\mathrm{Water\ Content}}$) of the wet fungal biomass obtained from the average of the triplicate samples. The total dry fungal biomass ($DM_{Fungal\ biomass}$) produced was then ascertained by subtracting the water content from the total wet biomass quantity.

$$\text{Water Content (\%)} = \left(1 - \frac{\text{DM}_{\text{Samples 1,2,3}}\ (\text{g})}{\text{WM}_{\text{Samples 1,2,3}}\ (\text{g})}\right) \times 100 \quad \text{(equation 1)}$$

$$\text{DM}_{\text{Fungal biomass}}\ (\text{g}) = \text{WM}_{\text{Fungal biomass}}\ (\text{g}) \times (100 - \overline{\text{Water Content}}) \quad \text{(equation 2)}$$

2.4 Extraction and treatment of natural polymers

Mycelial biomass was initially washed thrice with water and submerged for 5 min to remove any remaining molasses residue. The biomass was then blended for 5 min in 500 mL of water and the resulting suspension heated to 85°C for 30 min. The suspension was then cooled to 25°C and centrifuged at 9000 rpm for 15 min at 18°C. The resultant residue was resuspended in a 1 M NaOH solution for 3 h at 65°C. The suspension was cooled to 25°C and then neutralised (pH 7) by repeated centrifugation and redispersion of the residue in water.

Total dry polymer extract quantity ($DM_{Polymer\ extract}$) was assessed using the total wet polymer extract quantity and triplicate wet polymer extract samples dried and assessed as before for fungal biomass. These values were compared with values previously determined for the dry mass of fungal biomass grown, which allowed evaluation of the percentage conversion from fungal biomass to polymer extract (yield) for each species based on total dry biomass ($DM_{Fungal\ biomass}$) and total dry polymer extract ($DM_{Polymer\ extract}$). The polymer extract hydrogel was stored at 4°C until used further.

$$\text{Yield (\%)} = \frac{\text{DM}_{\text{Polymer extract}}\ (\text{g})}{\text{DM}_{\text{Fungal biomass}}\ (\text{g})} \quad \text{(equation 3)}$$

2.5 Preparation of nanopapers

Chitin-glucan or chitin-chitosan polymer extracts were suspended in 500 mL of water to allow for the production of nanopapers with a grammage of 50 g/m^2. Suspensions were vacuum filtered (VWR 125 mm qualitative filter paper 413, particle retention 5-13 µm), peeled and cold pressed for 5 min between blotting papers between metal plates under a 5 kg mass to remove excess moisture. The extracts were then hotpressed at 120°C for 15 min under 500 kg to achieve the final nanopapers. The entire nanopaper production process is summarised in **Figure 1.**

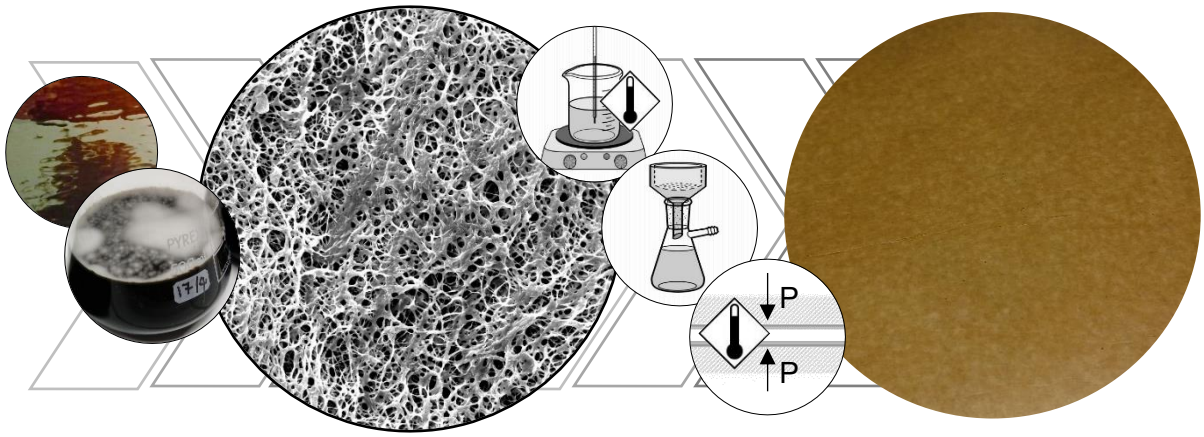

Figure 1. Nanopaper production process. A molasses medium is initially inoculated with the species of interest which grows to form a thick hyphal network. The biomass can then be treated using NaOH, the residue collected, vacuum filtered and hotpressed to produce the final nanopaper.

2.6 Morphological and elemental analysis of the nanopapers

Scanning Electron Microscopy (SEM) imaging and energy dispersive spectroscopy (EDS) elemental analysis of each nanopaper was performed using a Zeiss Supra 55 VP Scanning Electron Microscope with an Oxford X-Max^N 20 Energy Dispersive X-ray Spectrometer attached. An accelerating voltage of 30 kV was used. The EDS spectra were analysed using the AZtecEnergy EDS software. An average spectrum was obtained based on individual spectra from 12 different sites.

C, H, N, S and O elemental analysis was completed for triplicate 2 mg samples using a Eurovector EA 3000 CHNS-O elemental analyser. Complete digestion of phosphorus and (earth) alkaline elements in the samples was then completed by digestion in sulphuric acid (phosphorus), followed by mineralisation of the samples through combustion at 280°C (phosphorus) or 590°C (earth alkaline elements), with the residue dissolved in diluted nitric acid (pH ~3.0). P was determined through detection of ortho-phosphate using an Agilent Cary 8454 ultraviolet-visible diode array spectrophotometer and the K, Ca, Mg and Na content analysed using a PrinCE Crystal 310 Capillary Electrophoresis instrument, with detection registered using a TraceDec conductivity detector.

Carbohydrate analysis was carried out by high performance anion exchange chromatography (HPEAC). A 300 mg freeze dried sample was mixed with 3 mL of 72% sulfuric acid at 30°C for 60 min. The acid was then diluted with water to a 4% concentration and the mixture was placed in an autoclave at 121°C for 60 min. The HPEAC was performed on the previously diluted acid hydrolase with a Dionex ICS3000 chromatograph equipped with a CarboPac PA20 column. Sugar Recovery Standards (SRS) were prepared and pre-

treated in identical hydrolysis conditions prior to HPAEC analysis in order to analyse their recovery throughout the procedure.

2.7 Analysis of the molecular structure of the nanopapers

IR spectra were recorded using an Agilent Cary 630 FT-IR instrument with a single reflection diamond ATR-module and KBr optics (beam splitter). Three spectra were recorded from different portions of material to verify homogeneity. Spectra were recorded across the full accessible range from 4,000-400 cm^{-1}.

Solid state nuclear magnetic resonance spectroscopy (ssNMR) was performed on a Bruker Avance NEO 500 MHz wide bore system using a 2.5 mm magic angle spinning probe. Nanopapers were first frozen using liquid nitrogen, ground using a pestle and mortar and passed through a 75 µm sieve to produce a fine homogenous powder sample for analysis. The resonance frequency for ^{13}C NMR was 125.78 MHz, the MAS rotor spinning was set to 14 kHz. Cross-polarization was achieved by a ramped contact pulse with a contact time of 1 ms. During acquisition ^{1}H was high power decoupled using SPINAL with 64 phase permutations. The chemical shifts for ^{13}C are reported in ppm and are referenced external to adamantane by setting the low field signal to 38.48 ppm.

2.8 Physical and mechanical analysis of the nanopapers

The nanopapers were cut into dog bone shaped specimens (shape according to type 1BB, ÖNORM EN ISO 527-2, 2012) using a Zwick ZCP 020 Manual Cutting Press. Specimens had a parallel width of 2 mm and an overall length of 30 mm. The thickness of each specimen was determined using an AnyiMeasuring digital outside micrometer. Tensile tests were performed using a model 5969 Instron dual column universal testing system, equipped with a 1 kN load cell and a Gig ProE iMETRIUM non-contact video extensometer. Specimens were fixed between metal clamps using blotting paper to avoid perforation of the samples. Testing velocity was 1 mm/min with gauge length set to 12 mm. The elastic modulus (E) was analysed in the linear elastic region as a secant between strength values separated by 0.2 % strain. The tensile strength (σ) was calculated from maximum load and specimen cross-sectional area.

Nanopaper skeletal density was analysed for 10 replicate measurements using a Micromeritics AccuPyc II 1340 helium gas displacement pycnometry system with a 1 cm^3 chamber.

2.9 Surface energy analysis of the nanopapers

Advancing contact angles of polar (water) and non-polar (diiodomethane) droplets of test liquids on the nanopapers were determined using a Krüss DSA30 drop shape analyser. An initial contact angle measurement was recorded 0.5 s after dosing with double Sessile drops (3 µL drop of each test liquid), followed by 10 drops (0.2 µL each) dosed and measured with 0.5 s delay between each drop. A total of 100 measurements at 10 individual sites were recorded and screened individually for each nanopaper to ensure that droplet profiles were well formed and level. Contact angle and surface free energy were calculated using the Owens, Wendt, Rabel and Kaelble model[27] using the Krüss Advance software (v 1.5.1).

Surface free energy values were verified, and surface area assessed using a Surface Measurement Systems inverse gas chromatography (iGC) Surface Energy Analyser. The surface energy of mycelium-derived nanopapers was determined at 30°C and 0% RH. Nanopaper samples were cut and inserted into a measurement column (inner diameter 4 mm, outer diameter 6 mm). The specific surface area of the samples was initially determined by octane retention at various coverages, with specific surface area computed using the BET model from the peak maxima. A series of alkanes (hexane, heptane, octane, nonane, decane) were used for the determination of the surface energy in addition to polar probes dichloromethane, acetone, acetonitrile and ethyl acetate. The vapours were passed over the nanopaper samples and the retention times and volumes recorded. The total surface energy was computed using the Dorris and Gray method[28] based on the retention times and coverages of the various organic solvents from the peak maximums.

The ζ-potential of the mycelium-derived nanopapers was determined as a function of pH using an Anton Paar SurPASS electrokinetic analyser. The ζ-potential was measured in an adjustable gap cell (100 µm), with electrolyte solution (1 mM KCl) pumped through the cell at pressures steadily increased to 300 mbar. The pH was controlled by titrating 0.05 mol/L KOH and 0.05 mol/L HCl into the electrolyte solution and the ζ-potential determined from the streaming potential.

2.10 Thermal degradation analysis

Nanopaper thermal degradation properties were assessed using a TA Instruments Discovery TGA. Paper fragment samples of approximately 10 mg were placed in a platinum high temperature crucible and heated from 30°C to 1000°C at a heating rate of 20°C/min. Samples were tested in air and nitrogen atmospheres (both 25 mL/min).

3. Results and discussion

3.1 Dry mass and polymer yield of the mycelial biomass

Mycelial biomass typically had lower yields (biomass to chitin-glucan or chitin-chitosan polymer extract, corrected for the presence of inorganic Ca salts present in the extracts) (9.6% and 15.0% for *T. versicolor* and *M. genevensis*, respectively) than *A. bisporus* fruiting bodies (19.2%), except for *A. arbuscula*, which had a yield of 25.8% **(Table S1 supplementary material)**. Thus, fungal chitin sources typically had similar or slightly lower yields than processed crustacean chitin (8-33% yield).[29] This makes fungal chitin a viable, renewable, easily isolated, and abundant alternative to crustacean chitin, which can be rapidly produced on a large scale utilising heterotrophic growth on inexpensive agricultural by-products.[17] Nanopapers were then produced and characterised for each species. Mild alkaline extraction was utilised in this study to preserve the natural qualities of the polysaccharide-based fibers, with longer deproteination durations resulting in a higher degree of chitin deacetylation.[30-31] NaOH was utilised in this study, however extraction can also be achieved using other cost effective and environmentally sustainable methods utilising biological fermentation.[32] Bacteria that produce protease, such as *Serratia marcescens*, can be utilised to remove proteins, while bacteria producing lactic acid, such as *Lactobacillus paracasei*, can be used for harsher demineralisation if necessary.[33]

3.2 Chemical and elemental analysis of the polymer extract

Polymer extracts derived from *A. bisporus* fruiting bodies had significantly higher N (3.4 wt%), glucosamine (42.3 wt%) and glucose (52%) contents than those derived from mycelium (*A. arbuscula*, *M. genevensis* and *T. versicolor*), which indicated the presence of significantly higher chitin-chitosan and glucan fractions in these extracts **(Table 2 & 3)**. *M. genevensis* and *A. arbuscula* mycelium-derived polymer extracts had similar elemental N contents (1.7 wt% and 1.9 wt%, respectively), however, *M. genevensis* extracts had a significantly higher glucosamine content (22.8 wt%) than *A. arbuscula* extracts (13.7 wt%). This most likely resulted from the lower content of other carbohydrate compounds in extracts derived from *M. genevensis*. Both *A. arbuscula* and *M. genevensis* also contained significant amounts of glucose (42.2% and 43.3%, respectively) associated with glucan linked chitin. Polymer extracts produced from biopolymers extracted from *T. versicolor* had very low N concentrations (0.3 wt%); sugar analysis revealed that glucose was the prevalent sugar in these extracts (86.3%), most likely associated with large concentrations of glucan and a low glucosamine content. Polymers extracted from *A. arbuscula* and *M. genevensis* were also associated with significant quantities of arabinose, galactose and mannose, which are common sugars in many fungal exopolysaccharides.[34]

Table 2. Elemental analysis for fungal polymer extracts.

Species	Elemental composition (wt% of total mass)									
	C	H	N	O	S	P	K	Ca	Mg	Na
A. bisporus (fruiting body)	41.1	6.2	3.4	47.2	0.02	0.05	0.1	0.4	0.1	0.1
A. arbuscula (mycelium)	47.1	7.1	1.9	38.6	0.2	0.1	0.1	4.8	0.1	0.1
--- post H_2O_2 treatment	47.4	6.8	1.5	37.6	0.06	0.2	0.1	0.1	0.1	0.1
--- post HCl treatment	48.3	7.1	1.7	37.8	0.09	0.1	0.1	0.1	0.1	0.1
M. genevensis (mycelium)	47.8	7.5	1.7	38.7	0.08	0.1	0.9	4.8	0.1	0.2
T. versicolor (mycelium)	28.5	4.6	0.3	47.1	0.02	0.05	0.1	20.1	0.1	0.1

Table 3. Sugar composition based on fraction of total sugars present.

Species	Sugar composition (wt% of total sugars)					
	Arabinose	Galactose	Glucosamine	Glucose	Mannose	Other
A. bisporus (fruiting body)	0.1	0.3	42.3	52.0	5.1	0.2
A. arbuscula (mycelium)	4.3	33.1	13.7	42.2	5.9	0.8
--- post H_2O_2 treatment	3.5	25.4	18.8	45.0	6.7	0.6
--- post HCl treatment	4.1	27.0	17.9	43.6	6.9	0.7
M. genevensis (mycelium)	2.8	25.0	22.8	43.3	5.7	0.4
T. versicolor (mycelium)	0.0	0.0	12.3	86.3	0.5	0.9

ATR-FTIR spectroscopy **(Figure 2a)** confirmed the presence of chitin in most samples. -NH stretching was visible at 3228 cm^{-1}, in addition to an amide I band associated with C=O stretching at 1624 cm^{-1}. Amide II and III bands, resulting from -NH deformation, were also visible at 1544 cm^{-1} and 1320 cm^{-1}, respectively, with the amide III band confirming the presence of a secondary amide. The lack of -NH deformation-based interruption in the amide I signal, and the absence of an amide II band, supported the low concentrations of chitin in *T. versicolor* extracts. Conversely, strong amide I-III band signals in *A. bisporus* fruiting body derived polymer extracts supported the higher chitin content of these extracts. The carbohydrate backbone of the glucan and chitin polymer structure was also visible as an -OH band in all extracts at 3317 cm^{-1}, -CH bands at 2920 cm^{-1} and 2850 cm^{-1} and a C-O-C band at 1026 cm^{-1}.

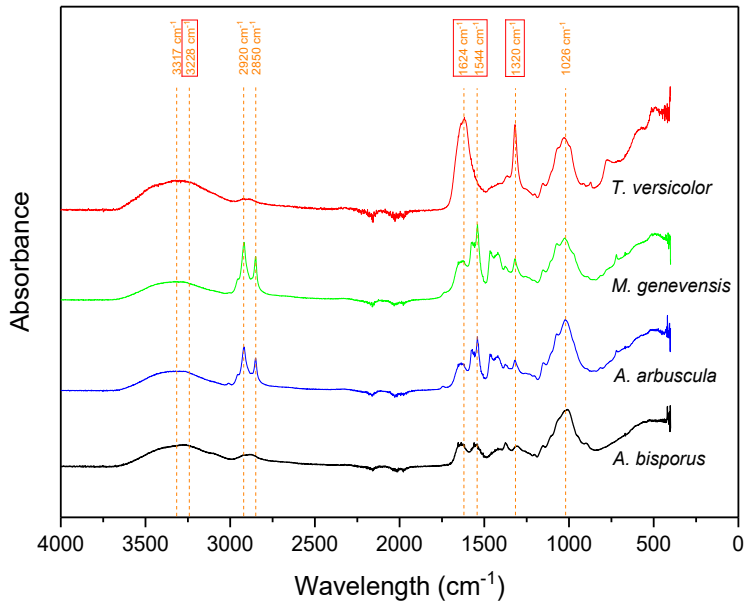

(a)

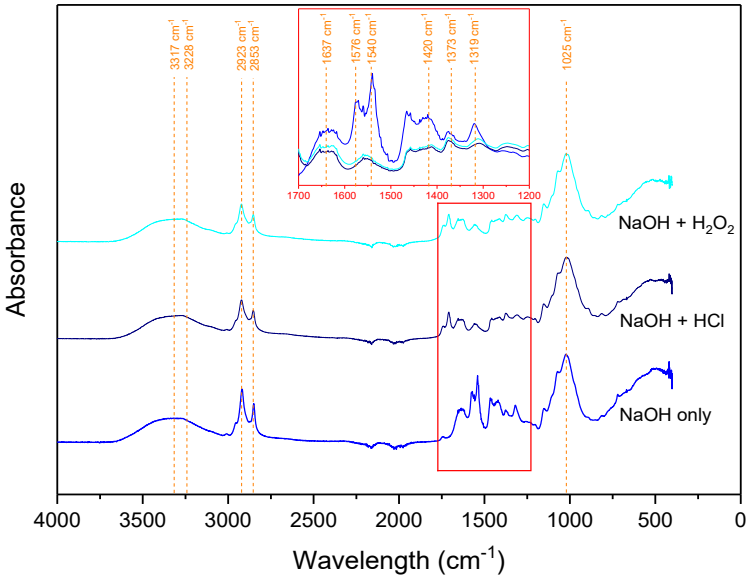

(b)

Figure 2. ATR-FTIR spectra for (a) nanopapers treated using only NaOH (mycelium-derived: *A. arbuscula* (blue), *M. genevensis* (green) and *T. versicolor* (red) and fruiting body derived: *A. bisporus* (black) nanopapers). Bands associated with -NH stretching and amides I-III are marked with red bounding boxes. (b) *A. arbuscula* nanopapers treated with NaOH + H_2O_2 (cyan) or NaOH + HCl (navy). Inset: magnification of bands associated with amides I-III.

Chitosan was also present in all polymer extracts, with ssNMR indicating that all extracts were at least partially deacetylated as confirmed by reduced -CH_3 and C=O signals at 22.5 ppm and 173.5 ppm, respectively **(Figure 3a)**. All samples exhibited C1-6 signals associated with the polysaccharide backbone as in chitin, chitosan and glucan between 55 ppm and 104 ppm. *A. bisporus* showed the strongest -CH_3 and C=O signals and thus the highest

fraction of acetylated monosaccharide units (30.8%) **(Table S2 supplementary material)**. This suggested that 30.8% of the sugars contained within this extract were chitin, with chitosan comprising a further 11.5% of the sugars present and other sugars representing 57.7% **(Table S3 supplementary material)**. *A. arbuscula* and *M. genevensis* still displayed signals indicating the presence of chitin, but the significantly reduced intensity and lower fractions of acetylated monosaccharide units suggested a lower chitin content (11.4% and 12.8% of the sugars present, respectively). This suggested the dominance of non-chitin polysaccharides (77.2-86.3% sugars other than chitin or chitosan) and a higher degree of deacetylation in these extracts, which were calculated to contain 2.3-10.0% chitosan **(Table S3 supplementary material)**. *T. versicolor* did not exhibit signals associated with -CH_3 and C=O, indicating a lack of chitin and the presence of chitosan or glucan instead. Measured ζ-potentials **(Figure S2 supplementary material)** supported these results with higher isoelectric points (IEP) associated with higher chitosan concentration papers and lower IEPs associated with papers containing more chitin. Pure chitin typically has an IEP of approximately 3.5,[35] while chitosan normally has an IEP of 7-9.[36-37] *M. genevensis* nanopapers had higher chitosan concentrations and IEPs of approximately 3.53. Conversely, nanopapers with lower chitosan concentrations, such as *A. arbuscula* and papers with higher chitin concentrations, such as *A. bisporus* had lower IEPs (3.19 and 2.87, respectively). The ζ-potentials of *T. versicolor* nanopapers could not be assessed as the samples disintegrated during the measurement. This was most likely due to the large concentrations of inorganic calcium salts in these nanopapers, which significantly compromised their physical and mechanical properties.

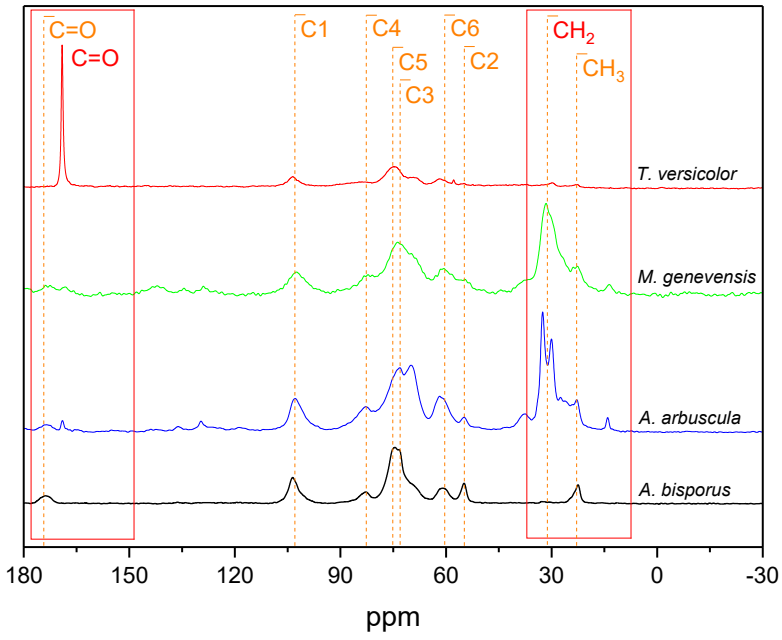

(a)

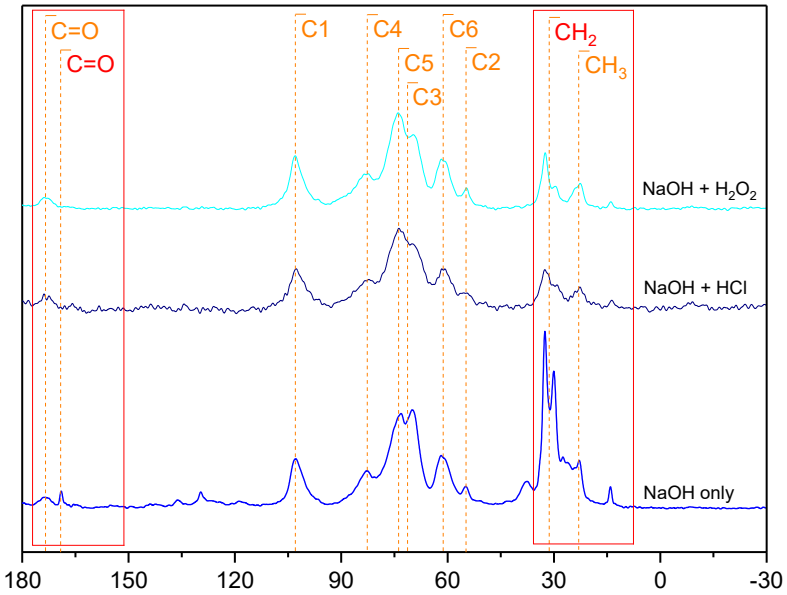

Figure 3. ^{13}C ssNMR spectra for (a) nanopapers treated using only NaOH (mycelium-derived: *A. arbuscula* (blue), *M. genevensis* (green) and *T. versicolor* (red) and fruiting body derived: *A. bisporus* (black) nanopapers) and (b) *A. arbuscula* nanopapers treated with NaOH + H_2O_2 (cyan) or NaOH + HCl (navy). Colours: orange text (C1-6, C=O, CH_3) is associated with chitin, red text (C=O, CH_2) is associated with organic lipid and inorganic Ca carbonate and oxalate contaminants. All peak integrals were referenced at C1.

All mycelium-derived polymer extracts only treated using NaOH contained large quantities of inorganics **(Table 2)**. Ca salts were especially prevalent in mycelium-derived samples (~5-20%), most likely derived from the molasses growth medium which contained 0.7 wt% Ca. Fungi growing in Ca rich environments typically contain Ca biomineralized in hyphae as calcite ($CaCO_3$) and calcium oxalate.[38] Biomineralization of hyphal filaments was visible using EDS point detect analysis, elemental composition mapping **(Figure S3 supplementary material)** and ssNMR results **(Figure 2a)**, which displayed a C=O peak associated with carbonate or oxalate at 169 ppm in all mycelium-derived papers, most prevalently in *T. versicolor*. ssNMR also indicated the presence of lipid residues in *A. arbuscula* and *M. genevensis*, with a -CH_2 peak at 31 ppm. However, it should be noted that lipid residues are not uncommon in chitin.[39]

A. arbuscula extract was subsequently selected for additional treatments to remove the organic and inorganic impurities detected based on its high conversion yield and growth rate compared to *M. genevensis* and *T. versicolor*. 1 M concentrations of H_2O_2 and HCl were used with a solid to solvent ratio of 1:15 (0.3 g polymer extract in 4.5 mL H_2O_2 or HCl solution) and constant stirring for 1 h at ambient temperature. Both H_2O_2 and HCl treatments did not significantly affect elemental or sugar composition, but were almost completely

effective in removing all inorganic Ca salts from the samples, with only trace quantities of Ca remaining after treatment **(Table 2)**. Lipid residue concentrations also decreased, indicated by significant reductions in the ssNMR -CH_2 peaks at 31 ppm **(Figure 3b)** and slightly more negative ζ-potentials between pH 5-10 resulting from greater chitin-based charge availability **(Figure S2 supplementary material)**. These reductions constituted ~22 wt% of the total polymer extract mass for H_2O_2 and ~23 wt% for HCl. ATR-FTIR spectra showed reductions in the amide II signals at 1576 cm^{-1} and 1540 cm^{-1} and the amide III signals at 1373 cm^{-1} and 1319 cm^{-1} associated with deacetylation of chitin in the treated nanopapers **(Figure 2b)**. The IEP of HCl treated papers also increased slightly and these papers had higher ζ-potentials at pH 2, supporting some degree of deacetylation on the paper surface **(Figure S2 supplementary material)**. ssNMR indicated that the fraction of acetylated monosaccharide units, and hence chitin content, increased from 11.4% to 14.0% following HCl treatment, potentially associated with glucan cleavage, and that the chitosan content of the sugars present also increased from 2.3% to 3.9% **(Tables S3 supplementary material)**. H_2O_2 treated extracts showed no signs of deacetylation based on ssNMR peaks and peak integrals, which indicated that the fraction of acetylated monosaccharide units (chitin content) increased from 11.4% to 17.2%, while chitosan content decreased from to 2.3% to 1.6% **(Table S3 supplementary material)**. H_2O_2 treated nanopapers also experienced a slight decrease in IEP from 3.19 to 2.99 **(Figure S2 supplementary material)**. This was most likely attributable to acid or carboxyl groups formed on the surface of H_2O_2 treated papers during oxidation.

3.3 Physical and mechanical properties of the nanopapers

Nanopapers produced from fibrils extracted from mycelia and fruiting bodies, exhibited dense surface morphologies lacking large pores or obvious fibrillation **(Figure 4a-d)**. *A. bisporus* fruiting body derived nanopapers exhibited a very densely bonded surface morphology of microfibrils containing very few Ca impurities **(Figure 4a)**. *A. arbuscula* had a marginally more visible fiber structure than *M. genevensis*, however both species appeared to have a hyphal filament structure biomineralized with Ca salts and interfaced with a surface layer of a lipid reside **(Figure 4b,c)**. This biomineralization and organic interfacing was confirmed by EDS mapping **(Figure S3 supplementary material)** but could be removed using H_2O_2 and HCl treatments, which exposed the hyphal filaments **(Figure 4e,f)**. Conversely, *T. versicolor* had a very fragmented surface morphology, which contained significantly higher (~4 times) concentrations of Ca salts and no visible hyphal filaments **(Figure 4d)**.

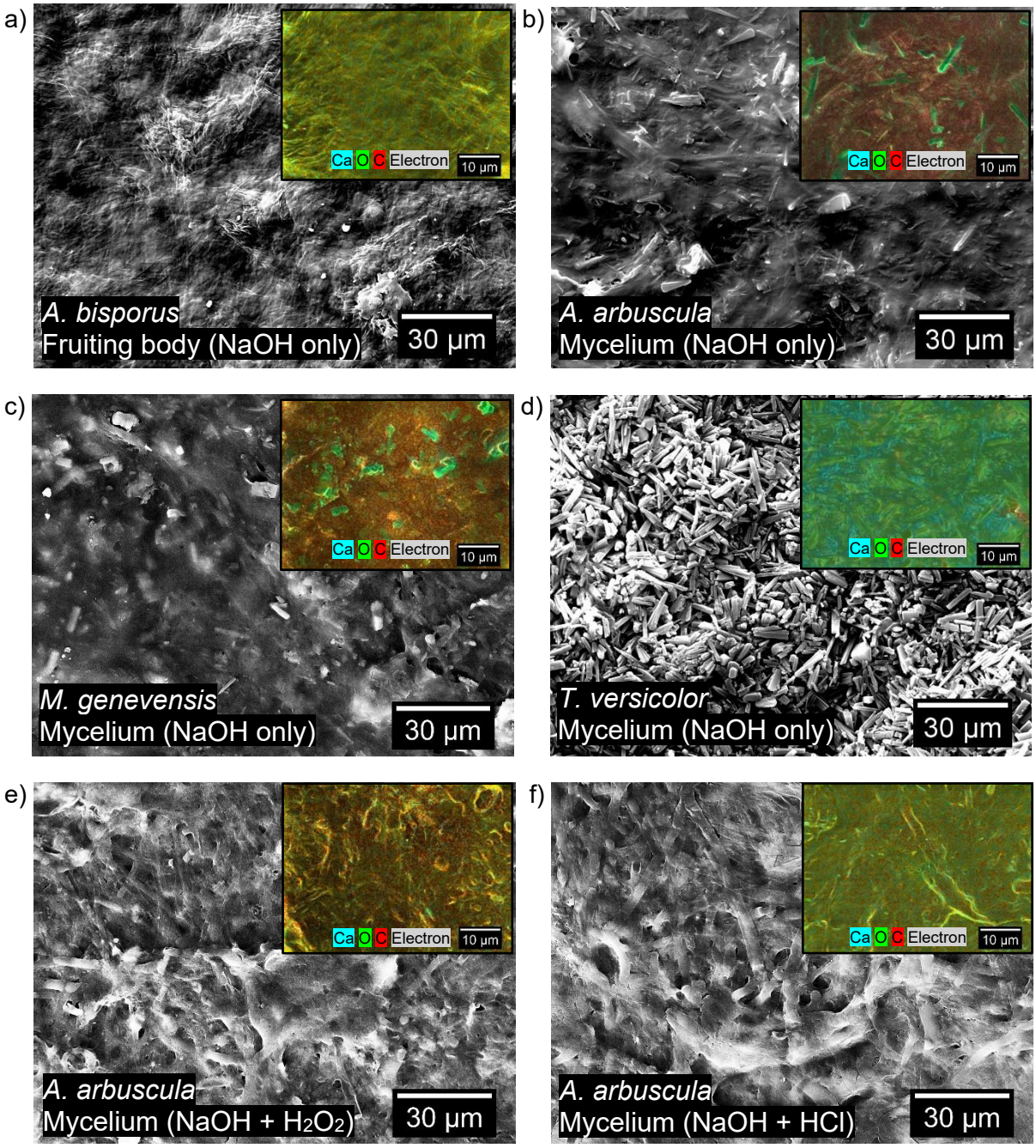

Figure 4. SEM micrographs (800x magnification) detailing the surface morphology of (a) *A. bisporus* fruiting body derived, (b) *A. arbuscula*, (c) *M. genevensis* and (d) *T. versicolor* mycelium-derived nanopapers treated with NaOH only, and *A. arbuscula* nanopapers treated with (e) NaOH + H_2O_2 or (f) NaOH + HCl.

The nanopapers produced from fibrils extracted from *M. genevensis* had the highest ultimate tensile strength of the mycelium-derived samples (24.7 MPa), being significantly stronger than *A. arbuscula* (16.0 MPa) and in particular *T. versicolor* (0.9 MPa) **(Figure 4)**. *M. genevensis* nanopapers were also more than twice as stiff as *T. versicolor* papers, which has an elastic modulus of 0.7 GPa, although *A. arbuscula* papers had a similar elastic modulus (1.8 GPa). The high chitin-chitosan contents of *M. genevensis* nanopapers

compared to *A. arbuscula* and *T. versicolor* is potentially responsible for these differences in mechanical performance. The presence of higher chitosan contents also explains the larger strain to failure of *M. genevensis* (1.5%), which was higher than *A. arbuscula* (1.1%) and *T. versicolor* (0.1%) **(Table 4)**.

A. bisporus fruiting body derived nanopapers had better mechanical performance than mycelium-derived nanopapers, with much higher ultimate tensile strengths (up to 97.6 MPa) and elastic moduli (up to 6.5 GPa) **(Figure 5)(Table 4)**. Their superior performance was most likely attributable to their significantly higher chitin and chitosan contents and the lack of Ca impurities in these papers. *A. arbuscula* mycelium-derived nanopapers were treated with H_2O_2 and HCl to remove Ca impurities and subsequently improve the purity of the polymer extracts used in the production of the mycelium-derived nanopapers. Despite successful removal of the Ca impurities, only a minor improvement in mechanical performance was achieved in the treated papers. The H_2O_2 treatment increased the fraction of acetylated monosaccharide units and provided some improvement in tensile strength (16.0MPa to 19.2 MPa) but the HCl treatment had no positive effect on tensile performance **(Table 4)**. It has been noted in literature that the acetyl group can contribute to the formation of hydrogen bonds with a higher acetylation degree providing greater resistance against fracture.[40] More significant improvements in performance may have been hindered by deacetylation of chitin in the nanopapers, glucan cleavage, a reduction in fibril-fibril bonding and increased porosity (reduced density) due to the removal of organic lipid residue that would otherwise bridge the fibrils **(Figure 4e,f)**.

Despite variations in tensile performance, the mycelium-derived nanopapers produced in this study matched or significantly outperformed all currently known mycelium-derived materials. Historically, mycelium composites have been characterised exclusively as foams, with low densities and elastic moduli, despite physical processing such as hot pressing **(Figure 6)**. The mycelium-derived nanopapers exhibited higher ultimate tensile strengths (up to 24.7 MPa) than mycelium composites (0.01-1.1 MPa)[3, 6] and mycelial biomass grown in controlled environments (5.1-9.6 MPa).[11] They also exhibited similar tensile performance to several advanced mycelium materials utilising genetic modification of the SC3 hydrophobin (Δsc3) gene and controlled growth environments to produce schizophyllan rather than glucan linked chitin (15.6-40.4 MPa).[11] However, the nanopapers produced in this study have the advantage of being able to be grown in any environment and being universally applicable to all fungal biomass rather than species and strain specific genetic modification. They were characterised as polymers, based on their density (1.3-2.0 g/cm^3) and elastic moduli (up to 1.9 GPa), which were also similar to or higher than existing mycelium composites (0.001-0.097 GPa), mycelial biomass (0.4-0.9 GPa) and Δsc3 mycelium materials (1.2-2.5 GPa).[3, 11]

Overall, mycelium-derived nanopaper mechanical performance was comparable to commercial copy paper and some plastics.[41]

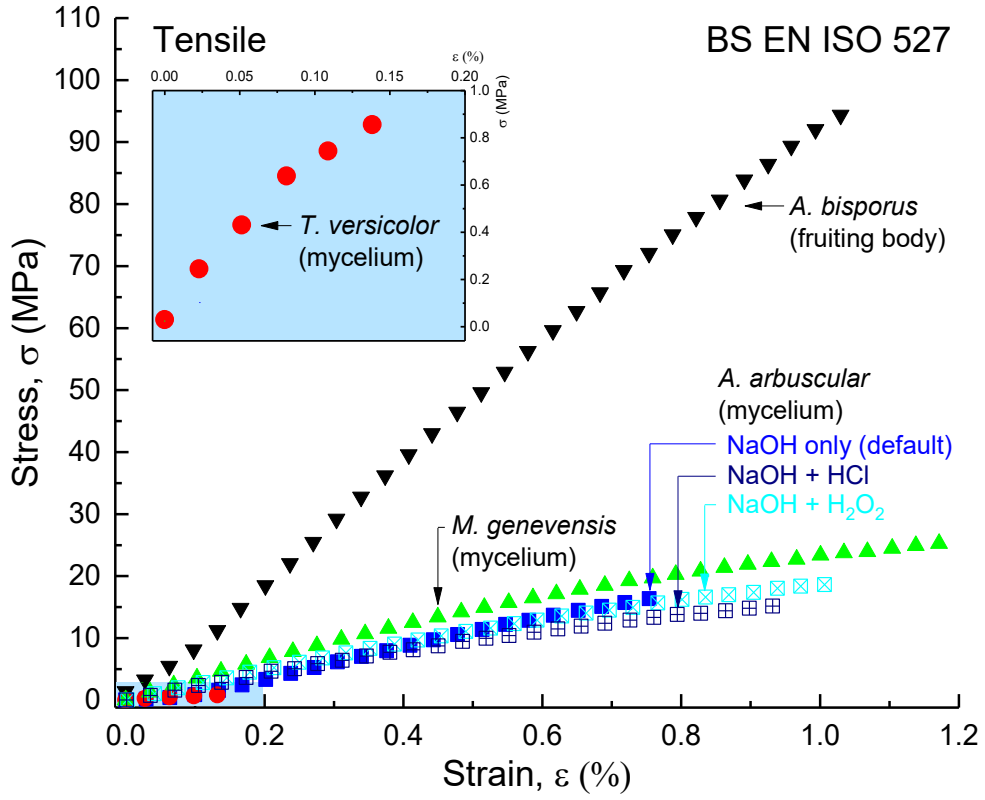

Figure 5. Tensile stress-strain curve for nanopapers treated using only NaOH (solid markers: mycelium-derived *A. arbuscula* (blue), *M. genevensis* (green) and *T. versicolor* (red) and fruiting body derived *A. bisporus* (black) nanopapers) and *A. arbuscula* nanopapers treated with NaOH + H_2O_2 (hollow cyan markers with diagonal cross) or NaOH + HCl (hollow navy markers with vertical cross). Inset: magnification of *T. versicolor* mycelium derived nanopaper stress-strain curve.

Table 4. Density (ρ), elastic modulus (E), ultimate tensile strength (σ_{UTS}) and strain to failure (ε_f) of nanopapers produced from fungal fruiting bodies and mycelium.

Species	**ρ (g/cm^3)**	**E (GPa ± SE)**	**σ_{UTS} (MPa ± SE)**	**ε_f (% ± SE)**
A. bisporus (NaOH only)	1.7 ± 0.003	6.5 ± 0.4	97.6 ± 8.3	1.8 ± 0.2
A. arbuscula (NaOH only)	1.4 ± 0.001	1.8 ± 0.4	16.0 ± 0.8	0.9 ± 0.3
--- NaOH + H_2O_2 treatments	1.2 ± 0.002	1.9 ± 0.1	19.2 ± 1.2	1.0 ± 0.1
--- NaOH + HCl treatments	1.3 ± 0.001	1.7 ± 0.1	14.3 ± 0.9	0.9 ± 0.1
M. genevensis (NaOH only)	1.3 ± 0.001	1.9 ± 0.2	24.7 ± 0.9	1.5 ± 0.1
T. versicolor (NaOH only)	2.0 ± 0.009	0.7 ± 0.01	0.9 ± 0.1	0.1 ± 0.01

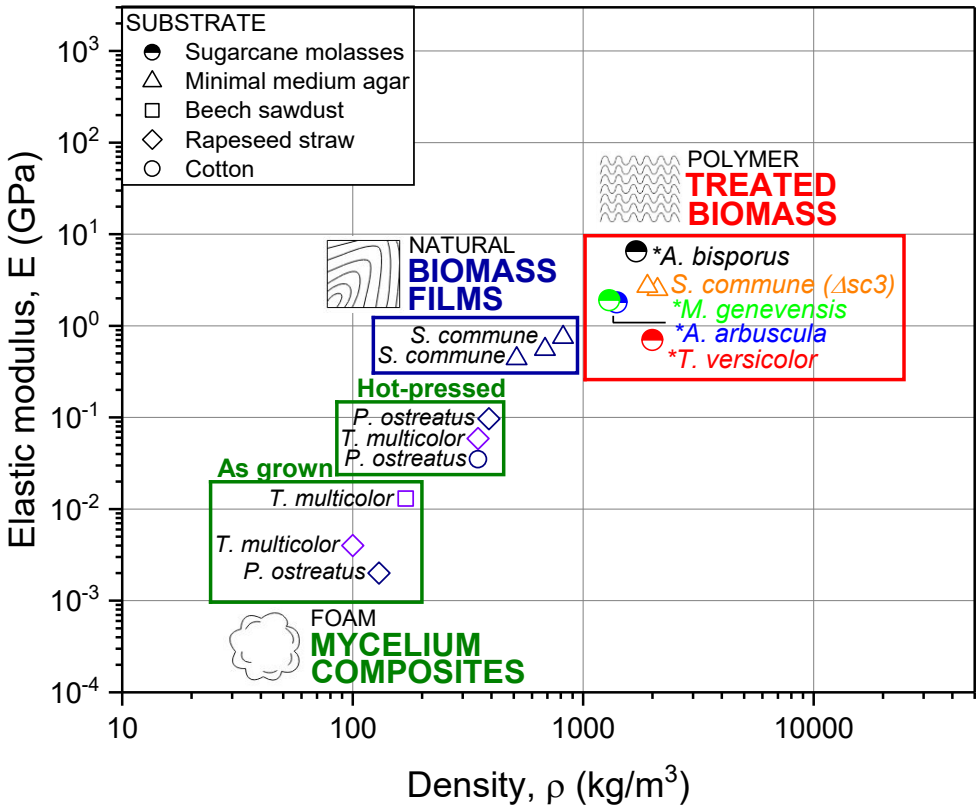

Figure 6. Comparison of the elastic modulus (GPa) and density (kg/m^3) of mycelium materials. The new chemically treated and hot-pressed nanopapers derived from mycelium and fruiting bodies produced in this study (*) are compared to existing as grown and hot-pressed mycelium composite materials, mycelial biomass and genetically modified Δsc3 biomass arranged by species and substrate. Data from Appels, et al.[3, 11] and Ashby, et al.[42]

3.4 Surface properties of the nanopapers

A further important aspect of mycelium-derived materials is their surface properties. Mycelium-derived nanopapers (*A. arbuscula* and *M. genevensis*) were hydrophobic, with high advancing water contact angles (~106° and ~101° respectively) compared to *A. bisporus* fruiting body derived nanopapers (~87°) and cellulose nanopapers (~19-90° depending on their lignin content)[43-45] **(Figure 7)**. The hydrophobicity of mycelium-derived materials has previously been noted, with static water contact angles from 115-122° reported.[6, 11] Both mycelium-derived papers also exhibited lower surface energies than *A. bisporus* fruiting body derived nanopapers (28-31 mJ/m^2 compared to 39 mJ/m^2) and had higher BET surface areas (1.7-2.1 m^2/g compared to 0.7 m^2/g) **(Figure 7)**. BET surface areas were assessed using inverse gas chromatography, which was also used to confirm the lower surface tensions. Total surface energies of 36 mJ/mm^2 and 40 mJ/mm^2 were recorded respectively for *A. arbuscula* and *M. genevensis* mycelium-derived nanopapers, while 46 mJ/mm^2 was recorded for *A. bisporus* fruiting body derived papers at 0.1 surface coverage **(Figure S5a supplementary material)**. Chitin and chitosan theoretically exhibit

slightly higher surface energy than other polysaccharides, such as cellulose and starch, due to the presence of amino and amide moieties.[46] The dispersive surface energy component of chitin or chitosan is approximately 30 mJ/m^2, a value typical of macromolecules, with a similar polar component contribution owing to the dominance of -OH surface groups (total surface energy of approximately 60 mJ/m^2) and a water contact angle of ~50°.[46] However, non-polar impurities have been noted to be responsible for lower polar surface energy components in less pure chitin.[47] Non-polar impurities responsible for the aroma of fungi, such as alcohols and acid derivatives[48] are probably responsible for the hydrophobicity and low surface energies of mycelium-derived nanopapers. In particular, the high concentrations of lipid residues in *A. arbuscula* and *M. genevensis* nanopapers were most likely responsible for the hydrophobic properties demonstrated by these papers. Hydrophobic properties could make mycelium-derived nanopapers useful for applications including coatings. *T. versicolor* mycelium-derived nanopapers did not support stable droplets, instead absorbing them on contact, and were consequently unable to be assessed.

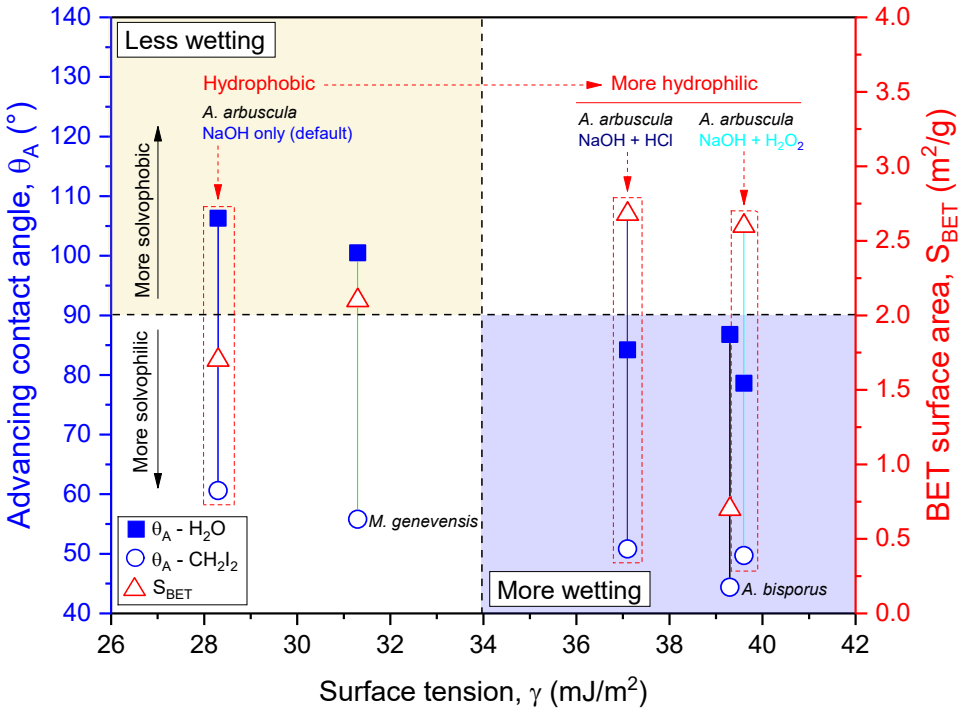

Figure 7. Advancing contact angle (blue markers, °), surface tension (mJ/m^2) and BET surface area (hollow red markers, m^2/g) measurements for *A. arbuscula* (blue connecting line) and *M. genevensis* (green connecting line) NaOH treated mycelium-derived nanopapers. *A. bisporus* fruiting body derived nanopapers (black connecting line) and *A. arbuscula* NaOH and H_2O_2 (cyan connecting line) or HCl (navy connecting line) treated nanopapers are also displayed, with the transition between hydrophobic and hydrophilic properties following HCl or H_2O_2 treatment marked in red. *T. versicolor* has been omitted from this figure as it was unable to be tested.

A. arbuscula mycelium-derived nanopapers treated with H_2O_2 and HCl displayed more hydrophilic behaviour than papers only treated with NaOH. The advancing water contact angles of these papers were significantly lower than NaOH only treated papers, with reductions from ~106° to ~79° or ~84° following H_2O_2 or HCl treatment, respectively **(Figure 7)**. The H_2O_2 and HCl treated papers also had higher surface energies than papers only treated with NaOH (37-40 mJ/m^2 compared to 28 mJ/m^2) **(Figure 7)**. This increase in surface energy was confirmed using inverse gas chromatography, which recorded a total surface energy increase following HCl or H_2O_2 treatment from 36 mJ/mm^2 to 46 mJ/mm^2 or 49 mJ/mm^2, respectively, at 0.1 surface coverage **(Figure S5b supplementary material)**. The increased hydrophilicity and surface tension of H_2O_2 and HCl treated papers most likely resulted from the removal of lipid residue present in *A. arbuscula* nanopapers only treated using NaOH. This reduction in lipid residue is also likely responsible for the higher BET surface areas of H_2O_2 or HCl treated samples. The more fibrous surface morphology of H_2O_2 and HCl treated papers, stripped of Ca salts, coupled with their lower water contact angles and higher surface tensions could potentially make these papers suitable for use as membranes in filtration systems.

3.5 Thermal degradation properties of the nanopapers

Mycelium itself typically exhibits a three-stage degradation process. Initially, free and chemically bonded water evaporates between 25-200°C (~5 wt%). A much larger mass loss then follows between 200-375°C, with onset of decomposition at ~280-290°C, associated with the degradation of organic constituents, such as proteins and polysaccharides (~70 wt%). Finally, from 450-600°C the primary residual char further degrades to form the final carbonaceous char reside.[49] Mycelium typically yields a char residue of approximately 23 wt% in a nitrogen atmosphere[6, 49] and demonstrates thermal degradation and fire reaction properties typical of organic materials.[50] All mycelium- and fruiting body derived nanopapers, except for *T. versicolor,* exhibited three stage thermal degradation typical of mycelium with char residues of ~20-23 wt% under a nitrogen atmosphere **(Figure 8a)**. *A. bisporus* fruiting body derived papers fully thermally decomposed in an air atmosphere, however *A. arbuscula* and *M. genevensis* mycelium-derived papers had an inorganic residue of ~8-9 wt%, attributable to their Ca content **(Figure 8a)**. *T. versicolor* mycelium derived nanopapers exhibited a multi-stage thermal degradation process up to 800°C and a final inorganic residue of ~34 wt% in air atmospheres, supporting the significant biomineralization of this species and the lower organic content of these nanopapers compared to the other mycelium-derived nanopapers **(Figure 8a)**.

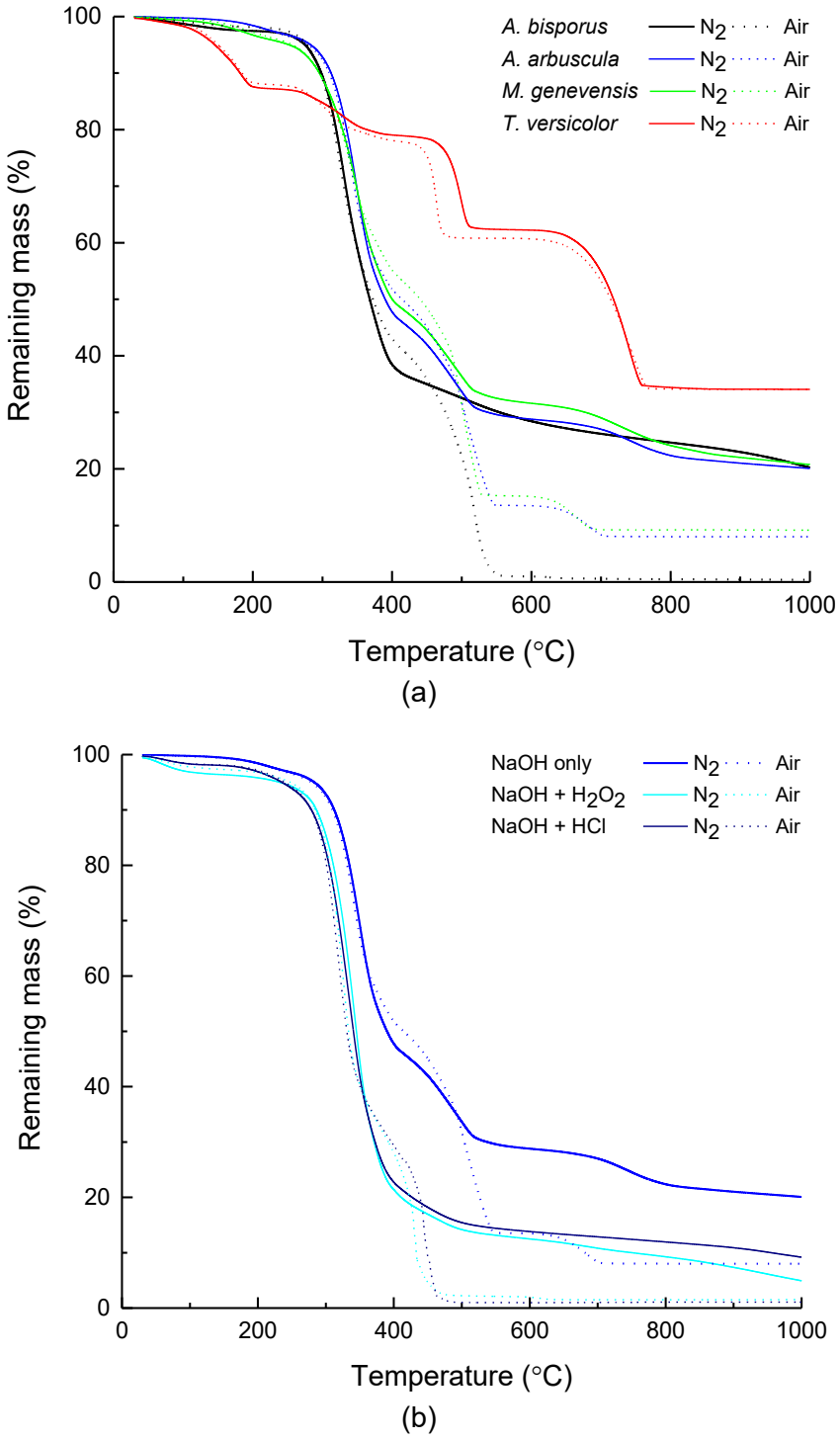

Figure 8. TGA-mass loss temperature curves for (a) nanopapers treated using only NaOH (mycelium-derived *A. arbuscula* (blue), *M. genevensis* (green) and *T. versicolor* (red) and fruiting body derived *A. bisporus* (black) nanopapers) and (b) *A. arbuscula* nanopapers treated with NaOH + H_2O_2 (cyan) or NaOH + HCl (navy).

A. arbuscula mycelium-derived nanopapers treated with H_2O_2 or HCl exhibited a three-stage thermal degradation process with a slight reduction in onset decomposition temperature. A reduction in char residue under a nitrogen atmosphere was also observed, with a drop from ~20 wt%, for papers only treated using NaOH, to ~4 wt% or ~9 wt% for papers treated using

NaOH + H_2O_2 or NaOH + HCl, respectively **(Figure 8b)**. H_2O_2 and HCl treated nanopapers fully thermally decomposed in an air atmosphere, with negligible inorganic char present above 600°C **(Figure 8b).** This verified the effectiveness of the H_2O_2 and HCl treatments in removing inorganic impurities from mycelium-derived nanopapers grown on Ca rich substrates, such as sugarcane molasses.

4. Conclusion

Fungal growth provides a low-cost method for on-demand generation of natural nanofibrils, such as chitin and chitosan, from agricultural wastes and by-products. These nanofibrils were obtained via mild alkaline extraction of a common mushroom reference and various species of fungal mycelium grown on the sugarcane by-product molasses and hot pressed to produce nanopapers. Mycelium-derived nanopapers were more hydrophobic than pure chitin and other natural polysaccharides, such as cellulose and starch, resulting from the presence of lipid residues within the nanopapers. Mycelium-derived polymer extract yields were competitive with crustacean chitin and nanopapers produced from the extracts exhibited much higher tensile strength than most existing mycelium materials, with comparable properties to paper and some plastics. Further hydrogen peroxide or hydrochloric acid treatments removed organic and inorganic impurities rendering the mycelium-derived nanopapers hydrophilic. Nanopapers derived from common mushrooms were hydrophilic, contained fewer lipid residues and inorganic contaminants than those derived from mycelium and had higher tensile performance. These variations in surface morphology, wettability and mechanical performance highlight the customisable properties of these cheap and environmentally sustainable materials making them potentially suitable for a wide range of applications, including coatings, membranes, packaging and paper.

Acknowledgments

This research was sponsored by an Australian Government Research Training Program Scholarship for M. Jones at RMIT University. The authors also wish to thank Stephan Puchegger and the University of Vienna Facility for Nanostructure Research for instrument access and technical assistance.

Supporting Information

Biomass and extract dry mass yields, associated water content and overall total dry polymer yield, energy-dispersive x-ray spectroscopy (EDS) spectra and elemental composition maps, zeta potentials as a function of pH, inverse gas chromatography (iGC) for total surface energy as a function of surface coverage, ^{13}C ssNMR peak integrals, fraction of acetylated

monosaccharide units, degree of acetylation and chitin and chitosan contents as a percentage of total sugars present.

Table of Contents Graphic

For Table of Contents Use Only. *Waste-derived Low-cost Mycelium Nanopapers with Tunable Mechanical and Surface Properties*, Mitchell Jones, Kathrin Weiland, Marina Kujundzic, Johannes Theiner, Hanspeter Kählig, Eero Kontturi, Sabu John, Alexander Bismarck, Andreas Mautner.

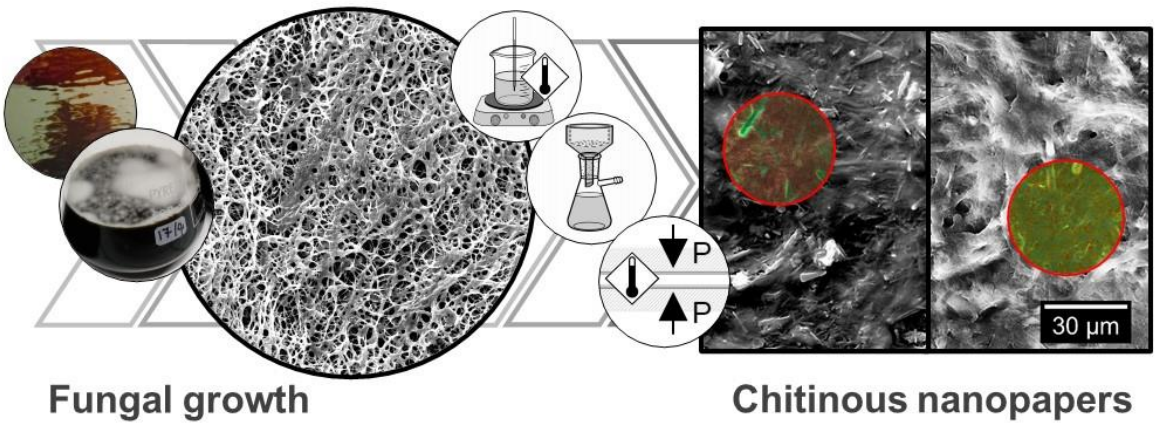

References

(1) Jones, M.; Huynh, T.; Dekiwadia, C.; Daver, F.; John, S., Mycelium Composites: A Review of Engineering Characteristics and Growth Kinetics. *Journal of Bionanoscience* **2017,** *11* (4), 241-257.

(2) Holt, G.; Mcintyre, G.; Flagg, D.; Bayer, E.; Wanjura, J.; Pelletier, M., Fungal mycelium and cotton plant materials in the manufacture of biodegradable molded packaging material: Evaluation study of select blends of cotton byproducts. *Journal of Biobased Materials and Bioenergy* **2012,** *6* (4), 431-439.

(3) Appels, F.; Camere, S.; Montalti, M.; Karana, E.; Jansen, K. M.; Dijksterhuis, J.; Krijgsheld, P.; Wösten, H. A., Fabrication factors influencing mechanical, moisture-and water-related properties of mycelium-based composites. *Materials & Design* **2019,** *161*, 64-71.

(4) Camere, S.; Karana, E., Fabricating materials from living organisms: An emerging design practice. *Journal of Cleaner Production* **2018,** *186*, 570-584.

(5) Karana, E.; Blauwhoff, D.; Hultink, E.; Camere, S., When the material grows: A case study on designing (with) mycelium-based materials. *International Journal of Design* **2018,** *12* (2), 119-136.

(6) Haneef, M.; Ceseracciu, L.; Canale, C.; Bayer, I. S.; Heredia-Guerrero, J. A.; Athanassiou, A., Advanced Materials From Fungal Mycelium: Fabrication and Tuning of Physical Properties. *Scientific Reports* **2017,** *7*, 41292.

(7) Pelletier, M. G.; Holt, G. A.; Wanjura, J. D.; Bayer, E.; McIntyre, G., An evaluation study of mycelium based acoustic absorbers grown on agricultural by-product substrates. *Industrial Crops and Products* **2013,** *51* (1), 480-485.

(8) Islam, M.; Tudryn, G.; Bucinell, R.; Schadler, L.; Picu, R., Morphology and mechanics of fungal mycelium. *Scientific Reports* **2017,** *7* (1), 13070.

(9) Abhijith, R.; Ashok, A.; Rejeesh, C. R., Sustainable packaging applications from mycelium to substitute polystyrene: a review. *Materials Today: Proceedings* **2018,** *5* (1, Part 2), 2139-2145.
(10) Arifin, Y. H.; Yusuf, Y., Mycelium Fibers as New Resource for Environmental Sustainability. *Procedia Engineering* **2013,** *53*, 504-508.
(11) Appels, F.; Dijksterhuis, J.; Lukasiewicz, C. E.; Jansen, K. M. B.; Wösten, H. A. B.; Krijgsheld, P., Hydrophobin gene deletion and environmental growth conditions impact mechanical properties of mycelium by affecting the density of the material. *Scientific Reports* **2018,** *8* (1), 4703.
(12) Kavanagh, K., *Fungi: Biology and Applications*. Wiley: Hoboken, NJ, 2005.
(13) Rinaudo, M., Chitin and Chitosan—General Properties and Applications. *ChemInform* **2007,** *38* (7), 603-632.
(14) Bamba, Y.; Ogawa, Y.; Saito, T.; Berglund, L. A.; Isogai, A., Estimating the Strength of Single Chitin Nanofibrils via Sonication-Induced Fragmentation. *Biomacromolecules* **2017,** *18* (12), 4405-4410.
(15) Webster, J.; Weber, R., *Introduction to Fungi*. Cambridge University Press: 2007.
(16) Ifuku, S., Chitin and chitosan nanofibers: Preparation and chemical modifications. *Molecules* **2014,** *19* (11), 18367-18380.
(17) Di Mario, F.; Rapana, P.; Tomati, U.; Galli, E., Chitin and chitosan from Basidiomycetes. *International Journal of Biological Macromolecules* **2008,** *43* (1), 8-12.
(18) Hassainia, A.; Satha, H.; Boufi, S., Chitin from Agaricus bisporus: Extraction and characterization. *International journal of biological macromolecules* **2018,** *117*, 1334-1342.
(19) Nawawi, W. M. F. W.; Lee, K.-Y.; Kontturi, E.; Murphy, R.; Bismarck, A., Chitin nanopaper from mushroom extract: natural composite of nanofibres and glucan from a single bio-based source. *ACS Sustainable Chemistry & Engineering* **2019,** *7* (7), 6492-6496.
(20) Jones, M.; Bhat, T.; Huynh, T.; Kandare, E.; Yuen, R.; Wang, C.; John, S., Waste-derived low-cost mycelium composite construction materials with improved fire safety. *Fire and Materials* **2018,** *42* (7), 816-825.
(21) Jones, M.; Huynh, T.; John, S., Inherent Species Characteristic Influence and Growth Performance Assessment for Mycelium Composite Applications. *Advanced Materials Letters* **2018,** *9* (1), 71-80.
(22) Griffin, D. H., *Fungal Physiology*. Wiley: Hoboken, NJ, 1996.
(23) Jones, M.; Lawrie, A.; Huynh, T.; Morrison, P.; Mautner, A.; Bismarck, A.; John, S., Agricultural By-product Suitability for the Production of Chitinous Composites and Nanofibers. *Process Biochemistry* **2019,** *80*, 95-102.
(24) American Type Culture Collection Fungi and Yeast Products. https://www.lgcstandards-atcc.org (accessed 3 August 2018).
(25) Bioresource Collection and Research Center Taiwan Fungal Flora Knowledge. http://www.bcrc.firdi.org.tw/fungi/index.jsp (accessed 3 August 2018).
(26) U.S. Department of Health and Human Services, Biosafety in Microbiological and Biomedical Laboratories. 2009.
(27) Owens, D. K.; Wendt, R., Estimation of the surface free energy of polymers. *Journal of applied polymer science* **1969,** *13* (8), 1741-1747.
(28) Dorris, G. M.; Gray, D. G., Adsorption of n-alkanes at zero surface coverage on cellulose paper and wood fibers. *Journal of Colloid and Interface Science* **1980,** *77* (2), 353-362.
(29) Gopalan Nair, K.; Dufresne, A., Crab shell chitin whisker reinforced natural rubber nanocomposites. 1. Processing and swelling behavior. *Biomacromolecules* **2003,** *4* (3), 657-665.
(30) Percot, A.; Viton, C.; Domard, A., Optimization of chitin extraction from shrimp shells. *Biomacromolecules* **2003,** *4* (1), 12-18.
(31) Li, J.; Revol, J. F.; Marchessault, R., Effect of degree of deacetylation of chitin on the properties of chitin crystallites. *Journal of Applied Polymer Science* **1997,** *65* (2), 373-380.

(32) Arbia, W.; Arbia, L.; Adour, L.; Amrane, A., Chitin extraction from crustacean shells using biological methods–a review. *Food Technology and Biotechnology* **2013,** *51* (1), 12-25.
(33) Jung, W.; Jo, G.; Kuk, J.; Kim, Y.; Oh, K.; Park, R., Production of chitin from red crab shell waste by successive fermentation with Lactobacillus paracasei KCTC-3074 and Serratia marcescens FS-3. *Carbohydrate Polymers* **2007,** *68* (4), 746-750.
(34) Mahapatra, S.; Banerjee, D., Fungal exopolysaccharide: production, composition and applications. *Microbiology insights* **2013,** *6*, 1-16.
(35) Wysokowski, M.; Klapiszewski, Ł.; Moszyński, D.; Bartczak, P.; Szatkowski, T.; Majchrzak, I.; Siwińska-Stefańska, K.; Bazhenov, V. V.; Jesionowski, T., Modification of chitin with kraft lignin and development of new biosorbents for removal of cadmium(II) and nickel(II) ions. *Mar Drugs* **2014,** *12* (4), 2245-2268.
(36) Gouda, M.; Elayaan, U.; Youssef, M. M., Synthesis and Biological Activity of Drug Delivery System Based on Chitosan Nanocapsules. *Advances in Nanoparticles* **2014,** *3* (4), 148.
(37) Swain, S.; Dey, R.; Islam, D. M.; Patel, R.; Jha, U.; Patnaik, T.; Airoldi, C., Removal of Fluoride from Aqueous Solution Using Aluminum-Impregnated Chitosan Biopolymer. *Separation Science and Technology* **2009,** *44* (9), 2096-2116.
(38) Burford, E. P.; Hillier, S.; Gadd, G. M., Biomineralization of fungal hyphae with calcite (CaCO3) and calcium oxalate mono-and dihydrate in carboniferous limestone microcosms. *Geomicrobiology Journal* **2006,** *23* (8), 599-611.
(39) Reid, D. G.; Mason, M. J.; Chan, B. K.; Duer, M. J., Characterization of the phosphatic mineral of the barnacle Ibla cumingi at atomic level by solid-state nuclear magnetic resonance: comparison with other phosphatic biominerals. *Journal of the Royal Society Interface* **2012,** *9* (72), 1510-1516.
(40) Cui, J.; Yu, Z.; Lau, D., Effect of Acetyl Group on Mechanical Properties of Chitin/Chitosan Nanocrystal: A Molecular Dynamics Study. *International journal of molecular sciences* **2016,** *17* (1), 61.
(41) Crompton, T. R., *Physical testing of plastics*. Smithers Rapra: 2012.
(42) Ashby, M. F.; Shercliff, H.; Cebon, D., *Materials: engineering, science, processing and design*. Butterworth-Heinemann: 2018.
(43) Operamolla, A.; Casalini, S.; Console, D.; Capodieci, L.; Di Benedetto, F.; Bianco, G. V.; Babudri, F., Tailoring water stability of cellulose nanopaper by surface functionalization. *Soft matter* **2018,** *14* (36), 7390-7400.
(44) Wang, Q.; Du, H.; Zhang, F.; Zhang, Y.; Wu, M.; Yu, G.; Liu, C.; Li, B.; Peng, H., Flexible cellulose nanopaper with high wet tensile strength, high toughness and tunable ultraviolet blocking ability fabricated from tobacco stalk via a sustainable method. *Journal of Materials Chemistry A* **2018,** *6* (27), 13021-13030.
(45) Lee, K.-Y.; Quero, F.; Blaker, J.; Hill, C.; Eichhorn, S.; Bismarck, A., *Surface only modification of bacterial cellulose nanofibres with organic acids*. 2011; Vol. 18, p 595-605.
(46) Cunha, A. G.; Gandini, A., Turning polysaccharides into hydrophobic materials: a critical review. Part 2. Hemicelluloses, chitin/chitosan, starch, pectin and alginates. *Cellulose* **2010,** *17* (6), 1045-1065.
(47) Cunha, A. G.; Fernandes, S. C. M.; Freire, C. S. R.; Silvestre, A. J. D.; Neto, C. P.; Gandini, A., What Is the Real Value of Chitosan's Surface Energy? *Biomacromolecules* **2008,** *9* (2), 610-614.
(48) Wekesa, N.; Lilechi, D.; Sigot, A.; Cheruiyot, J.; Kamau, R.; Kisiangani, P., Volatile and Non-polar Chemical Constituents of Cultivated Oyster

Mushroom Pleurotus ostreatus. *International Journal of Pharmacognosy and Phytochemical Research* **2016,** *8* (3), 477-479.
(49) Jones, M.; Bhat, T.; Kandare, E.; Thomas, A.; Joseph, P.; Dekiwadia, C.; Yuen, R.; John, S.; Ma, J.; Wang, C., Thermal Degradation and Fire Properties of Fungal Mycelium and Mycelium-Biomass Composite Materials. *Scientific reports* **2018,** *8* (1), 17583.

(50) Jones, M.; Bhat, T.; Wang, C.; Moinuddin, K.; John, S. In *Thermal Degradation and Fire Reaction Properties of Mycelium Composites*, 21st International Conference on Composite Materials, Xi'an, China, Xi'an, China, 2017.